Available online at www.sciencedirect.com

ScienceDirect

IFAC PapersOnline CONFERENCE PAPER ARCHIVE

IFAC PapersOnLine 52-11 (2019) 103–109

Wire Arc Additive Manufacturing by Robot Manipulator: Towards Creating Complex Geometries

Linn Danielsen Evjemo *, **Geir Langelandsvik** **, **Jan Tommy Gravdahl** ***

* *Department of Engineering Cybernetics, NTNU, Trondheim, Norway (e-mail: linn.d.evjemo@ntnu.no)*

** *SINTEF Industry, Trondheim, Norway (e-mail: geir.langelandsvik@sintef.no)*

*** *Department of Engineering Cybernetics, NTNU, Trondheim, Norway (e-mail: jan.tommy.gravdahl@ntnu.no)*

Abstract: Additive manufacturing (AM) is the umbrella term that covers a variety of techniques that build up structures layer-by-layer as opposed to machining and other subtracting methods. It keeps evolving as an important technology in prototyping and the development of new devices. However, using AM on a larger scale is still challenging, as traditional methods require the AM machines to be larger than the manufactured structure. The research presented in this paper is a continuation of our work on assessing the possibility of large-scale robotic AM. The focus in this paper is the feasibility of large-scale AM of metallic materials by arc welding. A series of experiments with robotic arc welding using an ABB IRB2400/10 robot are presented and discussed. These experiment will help map some of the challenges that need to be addressed in future work.

Keywords: Additive manufacturing, manufacturing systems, robot programming, wire arc additive manufacturing, aluminium alloys, Inconel alloys

1. INTRODUCTION

Traditional methods for additive manufacturing (AM) require the AM apparatus to be larger than the component it is producing. This puts great limitations on the volume of the structures that can be built, as it is only practical to extend the size of the machine up to a point. These AM techniques also mainly use a strictly layer by layer approach in the building process, either top-down or bottom-up, making it impossible to build overhangs without including additional support structures that must later be removed. Combining deposition of material with the flexibility of a 6 degrees-of-freedom (DOF) robot manipulator could drastically increase the workspace. If the material was fast-curing, like that of the MX3D Resin project (Jorislaarman.com, 2015-2018), a 6 DOF robot manipulator could deposit material in almost any direction. This would make it possible to move away from the layer-wise approach, and thereby remove the need for support structures when building more complex shapes, which could potentially help save both time and money.

The experiments presented in this paper build on our earlier work with AM by robot manipulators (Evjemo et al., 2017), where necessary algorithms and components for a system combining AM methods and a robot manipulator were outlined. Some initial experiments were done, using a 6 DOF UR-5 robot combined with an air-pressure driven caulking gun and a relatively fast-curing adhesive. This apparatus was used to build a simple cup-structure in a spiralling trajectory, moving away from the layer-wise approach. This work showed that AM by robot manipulator is indeed possible, and mapped some of the challenges that had to be addressed in future work. A state-of-the-art review of large-scale AM was also presented in this paper (Evjemo et al., 2017), showing the increased interest in different forms of large-scale AM: Spanning from how AM technology can be used to construct buildings (Apiscor.com, 2017) or bridges (Mx3d.com/"Bridge", 2017), to how the technology can be used creatively in art and design.

AM of metallic materials by arc welding could be useful in a variety of industries, and has the potential to not only perform robotised welding but to build metal structures from scratch. In this paper the focus is therefore on wire arc additive manufacturing (WAAM), with a special focus on the modified metal inert gas welding method cold metal transfer (CMT). CMT is well-suited for WAAM due to a more stable arc reducing metal splattering (so-called 'fireworks'), and a reduced heat input refining the deposited micro-structure and reducing residual stresses and distortion (Cong et al., 2016). Two sets of experiments are presented in this paper: Building a thin-walled, quadratic box, and building a more complex box-shape with challenges related to intersections within layers. An important objective for the experiments was to make the build as continuous as possible, as this could both save time and make the structure less prone to deformations. As with the experiment in (Evjemo et al., 2017), the robot

2405-8963 © 2019, IFAC (International Federation of Automatic Control) Hosting by Elsevier Ltd. All rights reserved.
Peer review under responsibility of International Federation of Automatic Control.
10.1016/j.ifacol.2019.09.125

Fig. 1. **Experimental set-up:** ABB IRB2400/10 robot manipulator with welding equipment from Fronius.

path is based on translation-only motions, the orientation of the welding gun staying fixed.

2. AM WELDING EXPERIMENTS BY 6 DOF ROBOT MANIPULATOR

In collaboration with SINTEF Industry, experiments were done using a 6 DOF IRB 2400/10 robot manipulator from ABB Robotics (Abb.com, 2016-2018). Attached to the robot's end effector was a metal inert gas (MIG) weld gun using the CMT technology developed by Fronius. This was partially controlled by the program running on the robot, though some settings had to be adjusted manually. The experimental set-up is shown in fig. 1. The robot path could be programmed manually with the robot control pad, or using the programming language RAPID. Testing was done in the simulation software RobotStudio from ABB.

2.1 Experiment 1: Thin-walled, quadratic box

AM of larger components is traditionally very time consuming due to slow deposition of material relative to the size of the final component. To make AM by robot as efficient as possible, it was of interest to assess the effects of a continuous build, and to avoid a strictly layer-wise build with a wait time between each layer. The structure in the initial welding experiment was geometrically very simple: A 10×10 cm^2 square-box built on a horizontal surface, as shown to the left in fig. 2. The aim was initially to test how a structure built by continuous welding would correspond to the heat development during prolonged deposition, and examine the visual appearance after deposition in terms of irregularities and distortions. Arc initiation and termination create uneven material deposition during WAAM, as reported by (Martina et al., 2012). Therefore, it was desirable not to have breaks during the welding process.

Manual programming: The first welding experiments were done by manually programming the path using the robot's

Fig. 2. **Square-box:** Smoother layer transitions, blunter corners and longer sides clearly improved the visual appearance of the structure.

control pad. The structure was welded onto a metal surface of AA6082 T6 rolled aluminium plate, from hereon referred to as the base, and the welding material was the aluminium-silicon alloy AA4047 in Ø1.2 mm wire form. The path was created by manually jogging the robot to each of the four corners of a square with the correct dimensions and saving these corner positions. Using a variation of the RAPID-function MoveL (ABB Robotics, 2004-2010), the robot was programmed to move linearly between these corners.

The distance from the tip of the welding gun to the base was approximately 12 mm. The estimated height of each deposited welding bead, from hereon referred to as the layer height, was set to 1.8 mm. The robot's end effector would move vertically one layer height at the end of each layer. The amount of deposited material was determined by the wire-feed speed, as well as the welding gun's travel speed along its path. The travel speed was set to 9 mm/second, and this value was kept throughout the experiments. The first square-box build was done welding with a current of 62 A. The resulting structure is shown to the left in fig. 2, where the corner closest to the camera is the starting point, and the transition point between layers.

RobotStudio: In the second experiment, the path was programmed using the programming language RAPID, and simulated in RobotStudio. The square-box dimensions were changed from 10×10 cm^2 to 12×12 cm^2, which implied a longer deposition distance in each layer, yielding a longer cooling time of the deposited material. This could in turn reduce distorting and overheating in the built components.

In the first experiment there was an issue with accumulation of material in the point of the vertical height increase, as can be seen in fig. 2. The transition between layers were therefore modified: Instead for a vertical movement in a single point, the height increase was spread over a slope of two centimetres at the end of each layer, as shown in fig. 3.

The square-box was designed with sharp corners. However, the first experiment showed that this made the end effector stay slightly longer in the corner points while changing direction, which lead to unwanted material accumulation. The corners were therefore made blunter in the following experiments by changing the *zone data* variable in the code so that the corner points worked as fly-by points instead of stop points: The robot's end effector would never actually reach the corner point on its path, but instead start changing directions when it was within a certain distance

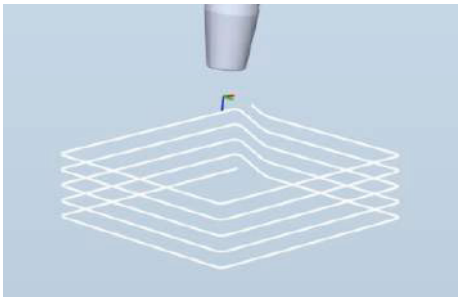

Fig. 3. **Slope between layers:** To avoid material accumulation, a smoother transition between layers was introduced, and the effect can be seen in fig. 2.

Fig. 4. **Continuous build:** Square-box structures with rounded corners and a smooth transition between layers.

of the corner point (ABB Robotics, 2004-2010). A value of *z1* meant that the tool centre point (TCP) could start changing directions 1 mm away from the fly-by point, while *z5* meant that the TCP could start changing direction 5 mm away from the point, and so on (Robotstudio.com, 2016). In this experiment, the zone data was set to *z5*. The initial build with these adjustments is shown to the right in fig. 2, and later builds with the same dimensions are shown in fig. 4.

2.2 Experiment 2: Flower-shape with opposing angles

One of the challenges that arise when building a thin-walled structure in a layer-wise manner is how to deal with intersections within the same layer (Ding et al., 2016). Continuous material deposition is desired for efficiency, but intersections in the robot's path within the same layer will then lead to deposition of material in the same point twice. Starting and stopping the welding process at each side of an existing bead is not considered to be a good solution due to the mentioned challenges regarding uneven material deposition at arc initiation and flame-out (Martina et al., 2012).

One solution to this problem is to altogether avoid crossings within the same layer. If the path within each layer can be traversed without passing the same point twice, it could be possible to design the path so that two opposite corner angles pass close enough together that they remelt and merge together, thereby creating what looks and works like an intersection. The method of opposite

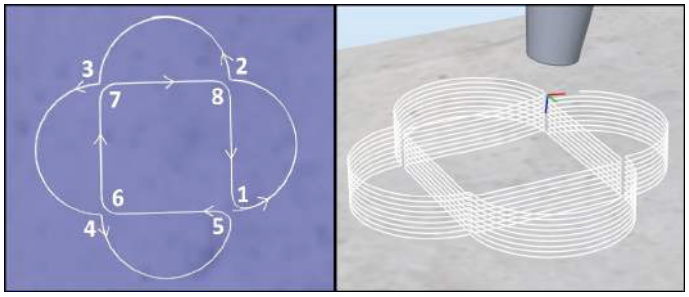

Fig. 5. **Opposite corners:** To avoid crossings within the same layer, the path was designed so that opposing corners merged together to create intersections in the final structure (Mehnen et al., 2011).

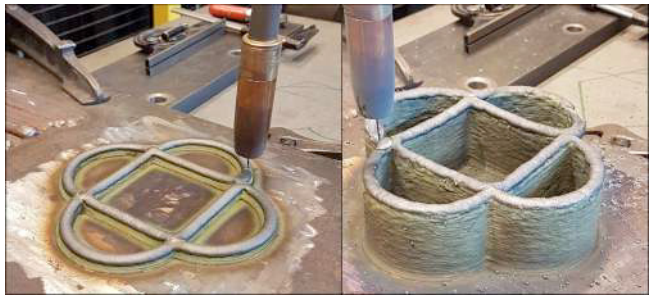

Fig. 6. **Inconel 625:** The flower structure built in Inconel 625 (4 layers to the left, 25 layers to the right). Fig. 10 shows the same structure after post processing.

angles described in (Mehnen et al., 2011) was tested for the thin-walled "flower"-shape, shown in the RobotStudio simulation in fig. 5. The pattern was repeated continuously for several layers. As with the box shown in fig. 2, the height increase between layers were done gradually over a slope of 2 cm at the end of each layer.

Three different materials were examined for the flower geometry. Tests were first done with the aluminium-silicon alloy AA4047 previously used to build the square-box. Further, the nickel-based alloy Inconel 625 was utilised, and some tests were done using another aluminium-silicon alloy, AA4043. The results from the former experiments were used to adjust the welding parameters in order to improve the final build.

The nickel- and aluminium-based alloys were used to assess the dependence of the physical properties of the welding metal when building. Compared to aluminium, Inconel 625 possess a much higher melting point (1350 °C) and higher thermal emissivity to air (Kobayashi et al., 1999). Welding with Inconel 625 requires higher energy input. Therefore, a pulsed MIG weld gun was preferred over CMT for this build, and the base plate was changed to black carbon steel. The as-deposited structure is shown in fig. 6, and the welding parameters are listed in table 2.

Lastly, a set of experiments were done trying to build the flower-shape in aluminium AA4043, using the experience from the previous experiments to attempt a successful build with a softer metal than the nickel-alloy. We wanted to weld the first few layers with an even higher heat input than before, so the last experiments with aluminium were done with pulsed metal inert gas (MIG) welding. This will be explained further in section 3. The welding parameters

Fig. 7. **Pulsed MIG:** The final flower structure built in aluminium AA4043. This build has 65 layers, and some grinding were performed to reduce material accumulation in the intersections.

are listed in table 3, and fig. 7 shows the most successful attempt.

3. RESULTS

Throughout these experiments, the accumulated experience regarding heat input and path design was implemented to help improve the following tests.

3.1 Experiment 1: Thin-walled square-box

Transitioning between layers by moving the welding gun vertically in a single point led to some unwanted material accumulation, as seen in fig. 2. As the aim was to see how feasible it was to build a structure by continuous welding, it was not an option to interrupt the welding procedure. This would in any case have lead to additional challenges related to the starting and stopping of the weld due to the difference in material deposition at the beginning and end of a welding bead (Mehnen et al., 2011). The gradual height increase over a slope introduced in the second square-box build, shown in the simulation in fig. 3, seemed to work well and was kept for the following experiments. Rounding off the corners seemed to solve the material accumulation problem there as well, as can be seen by comparing the corners of the structures in fig. 2.

The first, manual test with CMT with a current of 62 A seemed to overheat the structure, making the metal so hot and liquid that each layer became almost flat. The problem increased over time, making the walls of the structure uneven, as seen in fig. 2. Therefore, the heat input was reduced for the next builds, and the length of the walls was increased from 10 cm to 12 cm to allow for a longer cool-down period, resulting in the structure to the right in fig. 2. Fig. 4 shows additional builds of the square-box, where the material deposition could go on continuously until the structures were significantly taller than the first attempts.

3.2 Experiment 2: Flower-shape with opposing angles

Several experiments were done in order to build the structure shown in fig. 5, both in the aluminium alloys AA4047 and AA4043, and the nickel-based alloy Inconel 625.

Fig. 8. **Intersections:** First attempts at merging opposite corners together.

Opposing Angles: One challenge was to find an optimal distance between the corners in the path that needed to melt together, e.g. corner 3 and 7 in fig. 5. These corner parts of the path had the same fly-by point, but used different zone data, as explained in section 2.1. By changing how close to the fly-by point the end effector would move, it was possible to control the distance between the corners.

Two different builds in aluminium AA4047 are shown in fig. 8. The structure on the left had corners that ended up too close together, i.e. were too sharp. The material deposited in the opposing corners would slightly overlap, and this would accumulate over time, resulting in a height difference. The variation in the contact distance between the welding gun and the deposited structure due to the height difference in turn affected the material deposition, and the result was that the inner walls of the structure became slopes instead of straight walls. For the structure shown to the right in fig. 8, the corners were too blunt and far apart, so that the metal did not melt together as intended.

The flower-shape built in Inconel 625 (fig. 6) did not show the same issues related to the opposing corners as the aluminium structures in fig. 8. The material did not accumulate in the same way, and there were no clear signs of surface artefacts as the structure got hotter, and the build could go on continuously for 25 layers. The build was interrupted because the layer-height had been overestimated in the program. This meant that the distance between the welding gun and the welding surface increased for every layer. Thus, the Inconel 625 build was stopped after 25 layers when welding fireworks indicated that there were too long contact distance between the welding gun and the surface.

Three structures were built in the last experiment with aluminium AA4043. Height regulation was included in the program for the last test (3rd test table 3), so that the build could go on for much longer than any of the other tests. This last structure is shown in fig. 7.

Welding current and temperature: To make the weld adhere properly to the base, the first few layers of every structure had to be welded with a relatively high heat input. If not, the deposited material would just clump together in droplets, as shown in fig. 9, as the temperature was too low for the base metal and the deposited metal to properly melt together. To avoid deterioration of the structure due to excessive heat build-up, the heat input was reduced after the first few layers.

Fig. 9. **Low heat input:** Welding the first layers with a heat input that was too low made the deposited material clump together and not adhere properly to the base.

The welding parameters for the flower-shape experiments are listed in tables 1, 2 and 3. The changes in currents were done manually on the welding apparatus, not as part of the program running on the robot manipulator. To change the current, the program was interrupted by releasing the hold-to-run control, and then started again where it left off. This meant that there was a short break of 30-45 seconds between each layer with different currents.

Table 1. Welding param. for the tests building the flower-shape in aluminium AA4047.

Aluminium flower-shape (CMT welding)				
Layer	**Current**	**Wire feed sp.**	**Voltage**	**Layer h.**
1st test (approx. 12 × 12 cm)				
1-2	90 A	4.1 m/min	16.6 V	2 mm
2nd test (approx 16 × 16 cm)				
1-2	160 A	7.0 m/min	19.2 V	2 mm
3+	80	3.7 m/min	16.4 V	2 mm
3rd test (approx 16 × 16 cm)				
1-2	90 A	4.1 m/min	16.6 V	2 mm
3-10	60 A	2.9 m/min	16.1 V	2 mm
4th test (approx 16 × 16 cm)				
1-2	150 A	6.6 m/min	18.7 V	2 mm
3	100 A	4.5 m/min	16.9 V	2 mm
4-10	75 A	3.5 m/min	16.3 V	2 mm
8	100 A	4.5 m/min	16.9 V	2 mm
9-20	75 A	3.5 m/min	16.3 V	2 mm

4. DISCUSSION

Manually programming the welding process worked well enough for the simple square-box structure. However, it was inaccurate in the sense that the placement of the corners of the path was decided by how well the operator was able to aim manually. Editing existing scripts was tedious with this manual approach, e.g. moving the structure to another part of the base meant reprogramming

Table 2. Welding param. for the flower-shape build with Inconel 625.

Inconel 625 flower-shape (fig. 6 and 10)				
Layer	**Current**	**Wire feed sp.**	**Voltage**	**Layer h.**
1	185 A	7.9 m/min	15.3 V	2 mm
2	130 A	5.0 m/min	12.9 V	2 mm
3-4	120 A	4.4 m/min	12.6 V	2 mm
5-25	105 A	3.6 m/min	12.1 V	2 mm

Table 3. Welding param. for the tests building the flower-shape in aluminium AA4043.

Aluminium flower-shape (MIG pulsed welding)				
Layer	**Current**	**Wire feed sp.**	**Voltage**	**Layer h.**
1st test (approx. 16 × 16 cm)				
1-3	205 A	9.6 m/min	24.0 V	1.8 mm
4	149 A	6.8 m/min	20.7 V	1.8 mm
5	102 A	4.7 m/min	19.1 V	1.8 mm
6-25	72 A	3.5 m/min	18.4 V	1.8 mm
2nd test (approx. 20 × 20 cm)				
1	211 A	9.9 m/min	23.9 V	1.65 mm
2	151 A	6.9 m/min	20.9 V	1.65 mm
3	102 A	4.7 m/min	19.1 V	1.65 mm
4-30	72 A	3.5 m/min	18.4 V	1.65 mm
3rd test (With height reduction, approx. 20 × 20 cm)				
1	211 A	9.9 m/min	23.8 V	1.2 mm
2	151 A	6.9 m/min	20.9 V	1.2 mm
3	102 A	4.7 m/min	19.1 V	1.2 mm
4-65	72 A	3.5 m/min	18.4 V	1.2 mm

the entire path. It was therefore necessary to change to the more flexible way of programming the robot path in RAPID, which also made it simpler to create paths for more complicated structures. Furthermore, this made it possible to simulate and test the paths in RobotStudio.

Spreading the height increase between layers out over a short slope of a few centimetres seems like a good solution when working with a layer-by-layer approach. Because there is some slack in the optimal distance between the structure and the tip of the welding gun, this should work for any layer-wise structure as long as the layer height is relatively small compared to the length of the slope.

The solution for intersections used in these experiments, based on the work of (Mehnen et al., 2011), would of course demand that it is possible to traverse the entire path of one layer without the need for actual crossings. The flower-shape is so simple that one can see this path quite easily. More complex shapes would demand that we have an algorithm to help calculate the tool-path, e.g. the Medial Axis Transformation algorithm proposed by (Ding et al., 2014).

WAAM with aluminium AA4047 was challenging. The alloy's low melting temperature of 577 °C and high melt fluidity makes it vulnerable to overheating with prolonged deposition. The temperature vulnerability of building with aluminium proved more significant for smaller structures, which is to be expected as a larger area enable more heat dissipation to the base plate. In addition, a larger structure means that there is a longer cool-down period between each time material is deposited in the same point. Aluminium's inherent properties imply heat dissipation almost solely through conduction, and very low heat emission to air (Geng et al., 2017). In thin-wall building with an increasing number of layers, the heat dissipation gradually decreases due to longer conduction distance and decreasing temperature gradient through the thickness. Consequently, aluminium is especially vulnerable to overheating during prolonged deposition.

For the simple square-box structure with a large enough base area, continuous material deposition was possible for many layers without deterioration of the structure due to excessive heat build-up, as can be seen in fig. 4. It was

Fig. 10. **Post processing:** The Inconel 625 structure shown in fig. 6 after post processing. The opposing corners within each layer have merged together.

Fig. 11. **Grinding:** In the last test with aluminium AA4043 (fig. 7) some grinding was done every 10 layers or so in an attempt to avoid material accumulation in the intersection points.

more challenging to build the flower-shape. As explained in section 3.2, the inner walls of the flower structure became slopes instead of straight walls when welding with an aluminium-alloy. The inner walls are surrounded by heat, hampering heat dissipation. In addition, due to the high thermal conduction of aluminium, intersections become areas of heat accumulation. When a new layer is deposited in this high-temperature area, the cooling rate of the deposited metal goes down (i.e. solidification takes longer). Gravitational forces will flatten the liquid metal creating a wide, flat layer upon solidification. Further away from the intersection, deposited metal will solidify faster, creating a higher layer height. The discrepancy in layer height will accumulate over several layers, creating the slope seen in the flower component in fig. 7.

To avoid the poor surface appearance of the flower profile, a change of welding material from aluminium to Inconel 625 was performed. The nickel material had both higher melting point and thermal emissivity (Kobayashi et al., 1999). Consequently, more heat was dissipated to air creating a stable inter-pass temperature of the deposit. Without inter-sectional heat accumulation as with aluminium, the sloped wall phenomenon was avoided. Post processing shows that the corners did indeed melt together well enough to function as crossings within each layer, see fig. 10.

Different solutions were tested in order to successfully build the flower-shape without too much unwanted material accumulation in the opposite corners. There seemed to be a very fine balance between building the opposite corners too close together and too far apart, especially when working aluminium. Even the slightest accumulation of material in these intersection points had a large impact on the final result. In the test shown in fig. 7, some grinding was done to try and even this out, but the inner walls would still slope slightly.

With more experiments, it should be possible to optimise the distance between these kinds of opposite corners based on the structure's shape, size and material. The optimal distance varies a lot with the material and the welding parameters, because they determine the dimensions of the welding bead, which again determines how close together the opposite corners must be placed for them to merge. What worked best was a combination of rounded and sharp corners: Corner 5-8 in fig. 5 had zone data set to *z5*, while corner 2-4 had zone data set to *z1*. The merge between corner 1 and 5 was particularly challenging due to how the path was designed: The robot would stay longer in the same area, depositing more material, so the zone data in corner 1 was increased from *z1* to *z5*.

In the last aluminium build of the flower-shape, done with pulsed MIG welding, the path was altered so that the inner walls were built *before* the outer walls. The idea was that this should allow the heat to dissipate more quickly, as the inner walls would have time to cool down slightly before being enclosed by the heat from the outer walls. This might have had some effect on the first few layers, but as the structure grew taller, the height difference became negligible when considering heat flow.

The layer height for the Inconel 625 build was initially set to 2.0 mm, but as explained in section 3.2, this was too big, and the experiment had to be interrupted. The layer height should have been closer to 1.7 mm or thereabout. The program was adjusted so that the welding gun could be lowered during the last aluminium build, compensating for inaccuracies in assumed layer height. For the aluminium AA4043 build, the welding gun was lowered 21 mm over 65 layers, which is about 0.3 mm per layer. This implies that the layer height should be set to 0.9-1.0 mm instead of 1.2 mm for future experiments with pulsed MIG welding in aluminium for the given experimental setup.

5. CONCLUDING REMARKS

The work presented in this paper has shown that continuous WAAM shows promise when trying to build structures in this scale, though the results greatly depend on the building material. A smooth and gradual transition between layers works well to avoid deformations, and this solution could be kept for future experiments. Even so, building with a continuous height increase throughout the path should be considered, like what was done in the initial experiments described in (Evjemo et al., 2017). This would mean moving away from the layer-by-layer approach, avoiding the need for support structures.

If a layer can be built without actual crossings within the robot's path, intersections can be created through opposite corners (Mehnen et al., 2011), though it is clear that this is more challenging for aluminium than for harder materials such as Inconel 625. More research needs to be done to see how material properties can be used to calculate how close together such opposite corners should be placed, as this is

related to the dimensions of the welding bead at a given heat input, and the metal's melt fluidity and cooling rate.

As with the experiments presented in earlier work (Evjemo et al., 2017), these latest tests have all been done using translation-only robot paths with the welding gun placed perpendicular to a horizontal surface. Because each layer has to be vertically attached to the previous layer, these methods are limited when it comes to building structures with overhang, which will depend on support structures. The ABB IRB2400/10 robot manipulator has 6 DOFs, and can thereby reach every point in its workspace in an arbitrary orientation, so one of the next steps should be to use this flexibility to build more complex structures.

One way of doing this could be to change the orientation of the welded structure by rotating and tilting the welding surface, as shown in the work of (Panchagnula and Simhambhatla, 2018). The overlying objective of our research is to find methods that can be used to build larger structures, or to modify existing structures in industry. In such cases, having to change the orientation of the structure itself could be very limiting, so future work will therefore focus on controlling the orientation of the welding gun itself. When the welding gun is not placed vertically on the surface, it will be necessary to address challenges related to gravitational effects on the welding bead.

Monitoring the building process and designing control algorithms to correct for geometrical deviations in the structure should also be addressed in future work.

ACKNOWLEDGEMENTS

The work reported in this paper was based on activities within centre for research based innovation SFI Manufacturing in Norway, and is partially funded by the Research Council of Norway under contract number 237900. Mr. Morten H. Danielsen is acknowledged for his experimental guidance related to arc welding.

REFERENCES

ABB Robotics (2004-2010). Technical reference manual: RAPID Instructions, Functions and Data types.

Abb.com (2016-2018). IRB 2400. URL `https://new.abb.com/products/robotics/industrial-robots/irb-2400`. Accessed 2018-10-22.

Apis-cor.com (2017). Robotics in construction. URL `http://apis-cor.com`. Accessed 2019-06-07.

Cong, B., Ouyang, R., Qi, B., and Ding, J. (2016). Influence of cold metal transfer process and its heat input on weld bead geometry and porosity of aluminum-copper alloy welds. *Rare Metal Mat. Eng.*, 45(3), 606–611.

Ding, D., Pan, Z.S., Cuiuri, D., and Li, H. (2014). A tool-path generation strategy for wire and arc additive manufacturing. *Int. J. Adv. Manuf. Tech.*, 73(1-4), 173–183.

Ding, D., Shen, C., Pan, Z., Cuiuri, D., Li, H., Larkin, N., and van Duin, S. (2016). Towards an automated robotic arc-welding-based additive manufacturing system from CAD to finished part. *Comput. Aided Des.*, 73, 66–75.

Evjemo, L.D., Moe, S., Gravdahl, J.T., Roulet-Dubonnet, O., Gellein, L.T., and Brøtan, V. (2017). Additive manufacturing by robot manipulator: An overview of the state-of-the-art and proof-of-concept results. In *22nd IEEE ETFA, Cyprus*, 1–8.

Geng, H., Li, J., Xiong, J., and Lin, X. (2017). Optimisation of interpass temperature and heat input for wire and arc additive manufacturing 5A06 aluminium alloy. *Sci. Technol. Weld. Joi.*, 22(6), 472–483.

Jorislaarman.com (2015-2018). MX3D resin. URL `http://www.jorislaarman.com/work/mx3d-resin/`. Accessed 2018-10-22.

Kobayashi, M., Otsuki, M., Sakate, H., Sakuma, F., and Ono, A. (1999). System for measuring the spectral distribution of normal emissivity of metals with direct current heating. *Int. J. Thermophys.*, 20(1), 289–298.

Martina, F., Mehnen, J., Williams, S.W., Colegrove, P., and Wang, F. (2012). Investigation of the benefits of plasma deposition for the additive layer manufacture of Ti–6Al–4V. *J. Mater. Process Tech.*, 212(6), 1377–1386.

Mehnen, J., Ding, J., Lockett, H., and Kazanas, P. (2011). Design for wire and arc additive layer manufacture. In *Global Product Development*, 721–727. Springer.

Mx3d.com/"Bridge" (2017). Mx3d bridge. URL `https://mx3d.com/projects/bridge-2/`. Accessed 2019-06-07.

Panchagnula, J.S. and Simhambhatla, S. (2018). Manufacture of complex thin-walled metallic objects using weld-deposition based additive manufacturing. *Robot. Com.-Int. Manuf.*, 49, 194–203.

Robotstudio.com (2016). Rapid-ifdtechrefmanual: Zone data. URL `http://developercenter.robotstudio.com/BlobProxy/manuals/Rapid-IFDTechRefManual/doc576.html`. Accessed 2019-01-18.